Defects and carrier compensation in semi-insulating 4*H*-SiC substrates

N. T. Son,[1] P. Carlsson,[1] J. ul Hassan,[1] B. Magnusson,[1,2] and E. Janzén[1]
[1]*Department of Physics, Chemistry and Biology, Linköping University, SE-581 83 Linköping, Sweden*
[2]*Norstel AB, Ramshällsvägen 15, SE-602 38 Norrköping, Sweden*
(Received 13 June 2006; revised manuscript received 26 October 2006; published 12 April 2007)

Electron paramagnetic resonance (EPR) studies revealed that vacancies (V_C and V_{Si}), carbon vacancy-antisite pairs ($V_C C_{Si}$) and the divacancy ($V_C V_{Si}$) are common defects in high-purity semi-insulating (HPSI) 4*H*-SiC substrates. Their concentrations and some of their deep acceptor levels were estimated by EPR and photoexcitation EPR. The commonly observed thermal activation energies, $E_a \sim 0.8-0.9$ eV, ~ 1.1 eV, $\sim 1.25-1.3$, and ~ 1.5 eV, as determined from the temperature dependence of the resistivity, in different types of HPSI substrates were associated to different deep acceptor levels of V_{Si}, V_C, $V_C C_{Si}$, and $V_C V_{Si}$. The annealing behavior of these vacancy-related defects and their interaction at high temperatures (up to 1600 °C) in HPSI materials were studied. Carrier compensation processes were proposed to explain the observed change of the thermal activation energy due to high temperature annealing. V_C and $V_C V_{Si}$ were suggested to be suitable defects for controlling the SI properties whereas the incorporation of V_{Si} and $V_C C_{Si}$ during the crystal growth or processing should be avoided for achieving stable HPSI materials.

DOI: 10.1103/PhysRevB.75.155204 PACS number(s): 71.20.Nr, 61.72.Ji, 71.55.−i

I. INTRODUCTION

Silicon carbide (SiC) has the potential to replace conventional semiconductors in high-frequency high-power applications.[1] One of the key issues in the SiC technology is to develop high-quality SiC substrates. During the last few years, high-quality single-crystal SiC substrates with low densities of structural defects have been achieved.[2,3] However, in addition to the crystalline quality there are other requirements for the substrates to be used in power devices. In the power transistor chip, a passive parasitic capacitance, which is induced by the network of the metallized back side and fingers, wires, and lines on the epitaxial side, exists in parallel with the active capacitive part of the device, limiting the performance of the device at high frequencies. The parasitic capacitance must be minimized and the usual solution is to use semi-insulating (SI) substrates. This can be realized by incorporation of deep level centers to compensate shallow dopants. The SI properties can then be obtained but at a price of the presence of deep levels which may act as electron traps, worsening the performance of devices. Therefore, high-purity SI (HPSI) substrates with low concentrations of both shallow and deep centers are required.

In HPSI substrates grown by high-temperature chemical vapor deposition (HTCVD)[3–5] or by physical vapor transport (PVT),[6,7] intrinsic defects are believed to be responsible for the SI behavior of the material. Temperature dependence of the resistivity revealed several thermal activation energies E_a of $\sim 0.8-0.9$ eV, ~ 1.1 eV, $\sim 1.25-1.3$ eV, and ~ 1.5 eV in HPSI 4*H*-SiC materials grown by HTCVD and PVT.[4–7] Deep level transient spectroscopy (DLTS) data are not available due to the limitation of the technique with respect to SI materials. Nevertheless, the existence of these deep levels was confirmed by DLTS in *n*-type and *p*-type PVT substrates,[6] although the concentration of defects in HPSI materials can be different. Optical admittance spectroscopy (OAS) also revealed five deep levels with similar activation energies as determined from the resistivity data.[7] However, the information on the origin of defects and their concentrations cannot be obtained from OAS. Many defects in HPSI substrates have been observed by electron paramagnetic resonance (EPR) and optical techniques[8–11] but the defects related to different thermal activation energies have not been identified so far. The reduction of the resistivity (from $\sim 10^8-10^9\ \Omega$ cm to $\sim 10^5\ \Omega$ cm) and E_a (from $\sim 0.8-0.9$ eV to ~ 0.6 eV) was observed for some HTCVD substrates after annealing at 1600 °C (Refs. 4 and 5) and a similar instability of the SI properties was also found in earlier PVT SI substrates.[10] The reason that causes the instability of the SI properties in some types of substrates is still unknown. Identifying dominating defects in different types of substrates and understanding their roles in carrier compensation as well as their annealing behaviors are important for defect control in order to achieve HPSI materials with stable SI properties.

In this work, we used EPR to study defects in HPSI 4*H*-SiC substrates. Our investigation of a large number of samples showed that vacancies, divacancies and the carbon vacancy-antisite pairs are dominating defects in different types of HPSI 4*H*-SiC substrates. The energy positions of some acceptor levels of the divacancy and the carbon vacancy-antisite pair in the band gap of 4*H*-SiC were determined by EPR and photoexcitation EPR (photo-EPR). The high temperature annealing was performed on different sets of samples with different thermal activation energies to study the annealing behavior of vacancies and vacancy-related defects and their interaction as well as the stability of the SI properties. Based on the data obtained from EPR and annealing studies, we suggest a possible association between deep levels of vacancies and vacancy-related defects and commonly observed thermal activation energies.

II. EXPERIMENTAL DETAILS

Samples used in this work are *n*-type and HPSI 4*H*-SiC substrates grown recently by HTCVD and PVT techniques.

The substrates are characterized by low concentrations of the nitrogen (N) donors ($\sim 5-6\times 10^{15}$ cm^{-3}) and boron (B) acceptors ($\sim 1\times 10^{15}$ cm^{-3} and $\sim 3\times 10^{15}$ cm^{-3} for HTCVD and PVT substrates, respectively) as determined by secondary ion mass spectrometry (SIMS) (the detection limit of SIMS for N is ~mid-10^{15} cm^{-3}). EPR experiments were performed on ER200D and E580 X-band Bruker spectrometers. When illumination was needed to activate a certain charge state of the defect we used light from a 150 W xenon lamp and appropriate optical filters. For photo-EPR experiments we used a Jobin-Yvon 0.25 m grating monochromator with the step change in wavelength of 10 nm or 20 nm. A 200 W halogen lamp was used as excitation source with the operating power of ~150 W. The uncertainty in the determination of the photon energy can be ±0.03 eV (the slits of the monochromator was set at 1.5 mm). Annealing at temperatures above 1100 °C was performed in a CVD reactor with ~10 minutes at each temperature, but it is not isochronal due to the longer ramping times for heating up and cooling down in Ar ambient at higher temperatures. For annealing at lower temperatures (below 1100 °C), a conventional oven was used and the annealing time is about 1 hour. The activation energies were determined from the least-squares fits to the resistivity dependence on temperature as used in Refs. 4, 6, and 7, i.e., to $\rho \propto A\exp(E_a/kT)$ with ρ the resistivity and A a constant. The resistivity was determined from current-versus-voltage (I-V) measurements performed at high voltages (up to 1000 V) and in the temperature range 300–700 K using nickel contacts.

III. RESULTS AND DISCUSSION

A. Common defects and their concentration

EPR measurements were performed on a large number of different HPSI 4H-SiC samples. Based on the observed EPR centers and the measured thermal activation energy, the studied samples can be classified in three different sets: No. 1 with $E_a \sim 0.8-0.9$ eV, No. 2 with $E_a \sim 1.1-1.3$ eV, and No. 3 with $E_a \sim 1.5$ eV. Figures 1(a)–1(c) show the EPR spectra of the most common intrinsic defects in different types of HPSI 4H-SiC substrates measured at 77 K under illumination with light of photon energies ~2–2.8 eV for the magnetic field **B** along the c axis. As can be seen in Fig. 1(a), in samples with $E_a \sim 0.8-0.9$ eV, a strong EPR signal of the silicon vacancy (T_{V2a} center[12]) in the negative charge state (V_{Si}^-) (Ref. 13) is often detected together with weak signals of the $P6$ centers[14] and the positively charged carbon vacancy (V_C^+) (Ref. 15). The $P6/P7$ centers have recently been identified as the C_{3v}/C_{1h} configurations of the neutral divacancy ($V_C V_{Si}^0$).[16] In samples with $E_a \sim 1.1-1.3$ eV the $V_C V_{Si}^0$ signal has a similar intensity as in the sample set No. 1, whereas the V_{Si}^- signal is weaker and the V_C^+ signal is dominating [Fig. 1(b)]. In complete darkness, the samples with $E_a \sim 0.8-0.9$ eV and $E_a \sim 1.1-1.3$ eV show only a weak signal of the SI-1 center[10,11] as shown in the inset (i1) of Fig. 1. After exposing the samples in the sets No. 1 and No. 2 to light of photon energies larger than ~1.1 eV, the strong SI-5 signal can be observed in the dark [see the inset (i2) in Fig. 1]. The SI-5 center has recently been identified as the carbon vacancy-carbon antisite pair in the negative charge state ($V_C C_{Si}^-$) (Ref. 17). The $V_C C_{Si}^-$ signal is the dominating signal in samples with $E_a \sim 1.25-1.3$ eV and is somewhat weaker in samples with $E_a \sim 0.8-0.9$ eV. In samples with $E_a \sim 1.5$ eV, the signals of V_C^+ and $V_C V_{Si}^0$ are dominating. The V_C^+ signal was observed in the dark [see the inset (i3) in Fig. 1] whereas the $V_C V_{Si}^0$ signal could only be detected under illumination [Fig. 1(c)]. In the sample set No. 3, the EPR signals of V_{Si}^- and $V_C C_{Si}^-$ were not detected.

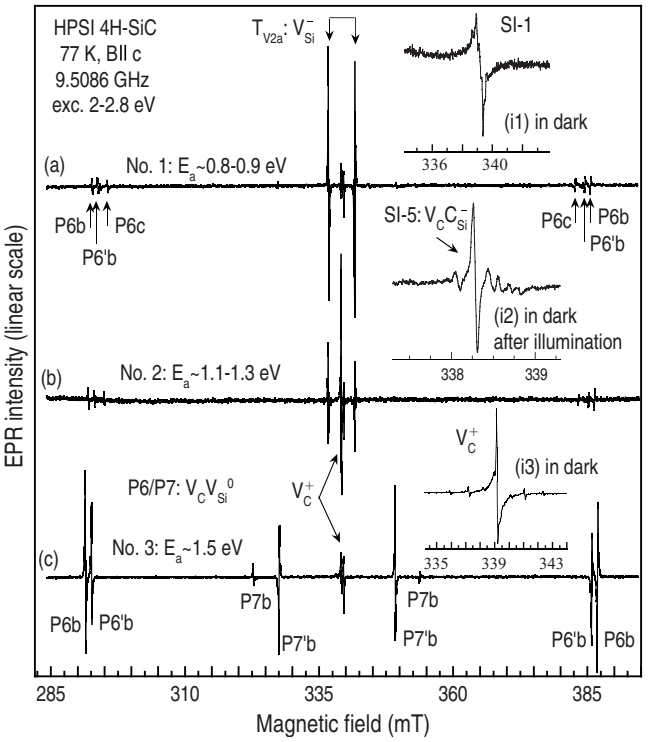

FIG. 1. EPR spectra observed under illumination with light of photon energies ~2–2.8 eV in different types of HPSI 4H-SiC substrates with the activation energy (a) $E_a \sim 0.8-0.9$ eV, (b) $E_a \sim 1.1-1.3$ eV, and (c) $E_a \sim 1.5$ eV. The insets show the EPR spectra in samples with $E_a \sim 0.8-1.3$ eV measured (a) in the dark and (b) in the dark after illumination, and (c) in samples with $E_a \sim 1.5$ eV measured in the dark.

In order to estimate the concentration of these intrinsic defects, we used samples with the same weight (110 mg) and compared the intensities of the EPR signals of defects in HPSI samples with the signal intensity of the N donor in a calibrated sample, which has the N concentration of n[N] $\sim 1\times 10^{16}$ cm^{-3} as determined by SIMS and by capacitance-versus-voltage measurements. In order to avoid the saturation effect which may occur with the EPR of the N donors at low temperatures, we performed EPR measurements at 77 K and optimized the conditions for detecting the maximum signal of N. The N spectrum measured in darkness is shown in Fig. 2(a). Depending on the Fermi level in different samples, the other spectra from intrinsic defects were detected either in darkness or under illumination with light of photon energies of ~2.0–2.8 eV. Figures 2(b) and 2(d) show EPR spectra of the $V_C C_{Si}^-$, V_C^+ and V_{Si}^- centers. The spectra were plotted with the same scale but shifted vertically so the comparison

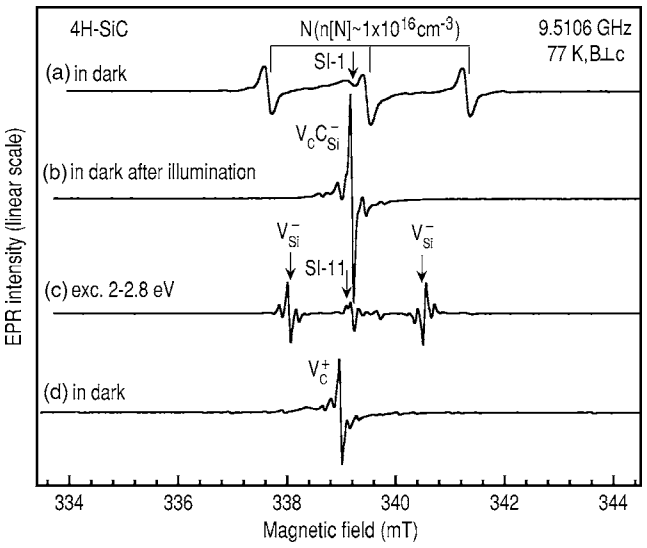

FIG. 2. EPR spectra in (a) n-type N-doped ($n[\mathrm{N}]\sim 1\times 10^{16}$ cm^{-3}) and (b)–(d) HPSI 4H-SiC samples (110 mg each) measured for $\mathbf{B}\perp\mathbf{c}$ at 77 K.

between their peak heights is possible. In all samples, the Fermi level was not suitable for detecting the $V_C V_{Si}^0$ signal in darkness so light illumination was needed to transfer the defects at least partly into the neutral charge states. In the case of measuring under illumination, only part of the total concentration of the defect being in the EPR active charge state may be measured. Therefore, the estimated concentration via the EPR intensity in such case can be lower than the real concentration. The divacancy concentration can be larger since the $V_C V_{Si}^0$ signal may represent only the fraction of the centers being in the neutral charge state (changed from the negative charge state by light illumination). Carlos and co-workers[18] estimated the concentration of these centers, which were believed to be $V_C C_{Si}^{2+}$ at that time, in HPSI 4H-SiC grown by PVT to be $>2\times 10^{16}$ cm^{-3}. We have carefully checked many samples and found that even in the sample with the strong $V_C V_{Si}^0$ signal, that the hyperfine interaction with three nearest neighboring C nuclei can be clearly detected and the inner Si hyperfine lines can be resolved, the concentration is only $\sim 6\times 10^{15}$ cm^{-3}. As we will show later in Sec. III C, in annealed samples with $n[V_C V_{Si}]\sim 1.5\times 10^{15}$ cm^{-3} the divacancy together with the B acceptors ($n[\mathrm{B}]\sim 3\times 10^{15}$ cm^{-3}) could not compensate the N donors ($n[\mathrm{N}]\sim 5\times 10^{15}$ cm^{-3}). We therefore believe that concentration of the divacancy estimated by EPR under light illumination is not much lower than the real concentration. The estimated concentrations of intrinsic defects in three different sets of HPSI samples are summarized in Table I. The values in Table I may not be considered as the absolute concentrations. As shown from Table I, the growth conditions that favor the incorporation of V_{Si} seem to suppress the formation of V_C and $V_C V_{Si}$ and result in SI materials with low activation energies (0.8–0.9 eV). Crystals grown under conditions favoring the formation of V_C and $V_C V_{Si}$ instead of V_{Si} and $V_C C_{Si}$ are characterized by higher thermal activation energies ($\sim$1.5 eV).

We also measured the concentration of intrinsic defects in some slightly n-type (with $E_a\sim 0.6$–0.7 eV and $n[\mathrm{N}]\sim 8\times 10^{15}$ cm^{-3}) and n-type ($n[\mathrm{N}]\sim 1$–2×10^{16} cm^{-3}) substrates. In these samples, the concentrations of V_{Si}, $V_C C_{Si}$, and $V_C V_{Si}$ are similar to those in substrates with $E_a\sim 0.8$–0.9 eV. The V_C signal is weak and is absent in some samples and its concentration may vary in the low-mid-10^{14} cm^{-3} range. In some Al-doped p-type ($n[\mathrm{Al}]\sim 4.8\times 10^{17}$–$4\times 10^{18}$ cm^{-3}) substrates grown by HTCVD, we observed a strong signal of V_C^+ similar to the case of HPSI substrates with $E_a\sim 1.5$ eV, whereas the V_{Si}^- and $V_C C_{Si}^-$ signals were absent.

The unidentified defects SI-1 [Fig 2(a)] and SI-11 [Fig. 2(c)] are observed in all n-type and HPSI samples. The SI-11 center have an isotropic g value of $g=2.0037$. The intensities of their EPR signals are not altered by electron irradiation, which is known to create intrinsic defects, indicating that they may be related to impurities. The concentrations of SI-11 center are estimated to be in the low-mid-10^{14} cm^{-3} ranges. The SI-11 signal does not change whereas the SI-1 signal increases its intensity after annealing at 1800 °C when the substrates already changed to n-type. This suggests that the SI-1 and SI-11 centers do not play an important role in carrier compensation.

B. Deep acceptor levels of vacancies and vacancy-related defects

In our previous photo-EPR experiments,[10] we observed an energy threshold of 1.75 eV for the appearance of the SI-5 (or $V_C C_{Si}^-$) signal. Those experiments were performed on an old HPSI 4H-SiC sample grown by PVT with high doping level of B ($\sim 1\times 10^{16}$ cm^{-3}). The similar increase of EPR signals of the shallow B acceptor and $V_C C_{Si}^-$ with the photon energy of the excitation indicated that the energy threshold of 1.75 eV is related to the transition from the shallow B acceptor level located at $\sim$0.27 eV above the maximum of the valence band, E_V, to the $(0|-)$ level of $V_C C_{Si}$. This places the

TABLE I. Concentrations of intrinsic defects in the sample sets Nos. 1–3 estimated by comparing the intensity of their EPR signals with that of the N signal in a calibrated sample with $n[\mathrm{N}]\sim 1\times 10^{16}$ cm^{-3}. Defects that are not detectable by our EPR experiments may have concentrations in the low 10^{14} cm^{-3} ranges.

Sample set	E_a (eV)	V_{Si} (cm^{-3})	$V_C C_{Si}$ (cm^{-3})	V_C (cm^{-3})	$V_C V_{Si}$ (cm^{-3})
No. 1	$\sim$0.8–0.9	$\sim 2.3\times 10^{15}$	$\sim 1\times 10^{15}$	mid-10^{14}	mid-10^{14}
No. 2	$\sim$1.1–1.3	$\sim 1\times 10^{15}$	~ 3–4×10^{15}	~ 2–3×10^{15}	mid-10^{14}
No. 3	$\sim$1.5	Not detectable	Not detectable	~ 3–4×10^{15}	~ 5–6×10^{15}

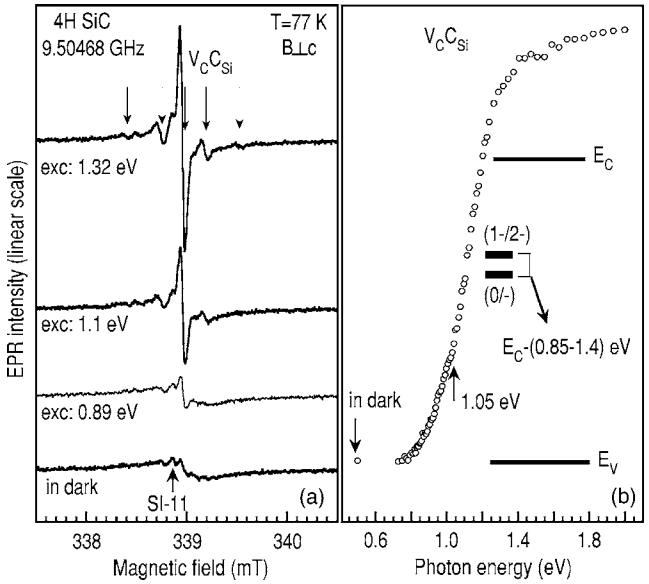

FIG. 3. Photo-EPR of $V_CC_{Si}^-$ in 4*H*-SiC: (a) EPR spectra in slightly *n*-type 4*H*-SiC measured in the dark and under illumination with light of photon energies of ~0.89 eV, ~1.1 eV, and ~1.32 eV. (b) The spectral dependence of the EPR intensity of the $V_CC_{Si}^-$ signal on the photon energy of excitation light.

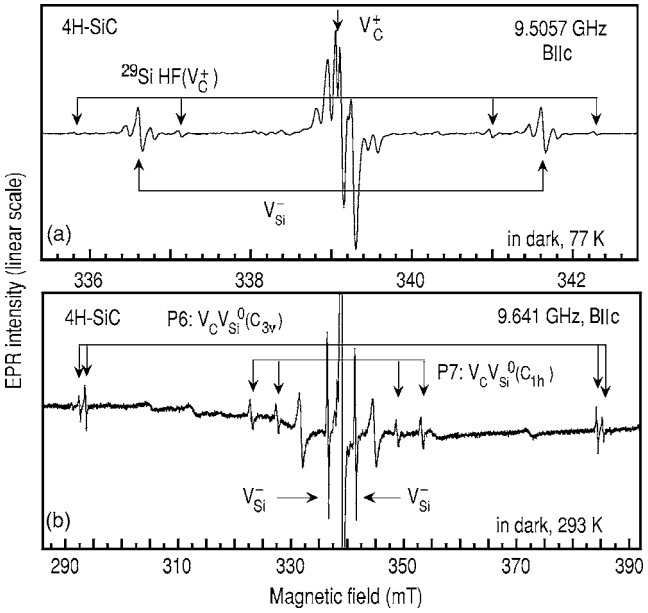

FIG. 4. EPR spectra in an HPSI sample irradiated with electrons (dose ~2×10^{18} cm^{-2}) and annealed at 850 °C measured in the dark at (a) 77 K and (b) 293 K.

(0|−) level of V_CC_{Si} to be at ~ (1.24 eV+ possible Franck-Condon shift[19,20]) below the conduction band minimum, E_C. In this work, we used a slightly *n*-type 4*H*-SiC sample grown by HTCVD for photo-EPR study to estimate the energy separation from this level to the conduction band minimum. In this sample, the EPR signals of $V_CC_{Si}^-$ and V_{Si}^- are dominating. EPR spectra measured in the dark and under illumination with light of different photon energies are shown in Fig. 3(a). The spectral dependence of the intensity of the $V_CC_{Si}^-$ signal on the excitation energy is shown in Fig. 3(b). The data corresponding to photon energies lower than ~0.73 eV (wavelength ~1700 nm) could not be collected due to the lack of optical filters in this spectral region. However, the spectrum measured under illumination with light of wavelength 1700 nm is very similar to that measured in darkness, indicating that there is no change of the EPR intensity induced by light of photon energies lower than 0.73 eV. The $V_CC_{Si}^-$ signal starts increasing at a photon energy of ~0.85 eV. It slowly increases with increasing the photon energy in the range 0.85–1.05 eV and quickly approaches a saturation at ~1.35–1.4 eV [Fig. 3(b)]. The spectral dependence of the EPR intensity can be explained as follows. The slow increasing region 0.85–1.05 eV may correspond to indirect transitions which removes electrons from the (1−|2−) level of V_CC_{Si} to some intermediate states and turns a part of the defect to the single negative charge state being detected by EPR. The spectral region 1.05–1.35 eV is possibly related to the direct transition from the (1−|2−) level to the conduction band with the threshold at ~1.05 eV. When the photon energy can induce a direct transition from the (0|−) level to the conduction band, the $V_CC_{Si}^-$ signal approaches a saturation corresponding to a steady state between the excitation and recombination processes, keeping a part of the total concentration of the defect in the negative charge state. Thus we can estimate that the transition from the (0|−) level to the conduction band including a Franck-Condon shift is not more than 1.4 eV. Combining with the photo-EPR results from Ref. 10, we estimate the (0|−) level of V_CC_{Si} to be in the region 1.24–1.4 eV below the conduction band.

In our studies of the temperature dependence of the resistivity, the activation energies of E_a~1.28 eV and E_a ~1.1 eV were found in HPSI samples with dominating signals of $V_CC_{Si}^-$ and V_C^+ (some of the samples with E_a ~1.28 eV and E_a~1.1 eV used in this work were indeed cut from different parts of the same wafer). In the sample used in our photo-EPR experiment, the signal of V_C^+ was not observable. The activation energy E_a~1.28 eV falls well in the energy region of 1.24–1.4 eV determined by photo-EPR and is possibly related to the (0|−) level of V_CC_{Si}. The (−|2−) level of V_CC_{Si} was predicted by supercell calculations to be at ~(E_C−1.0) eV and ~(E_C−0.9) eV for the cubic and hexagonal configuration, respectively.[17] This is in agreement with our photo-EPR observation. Considering the ionization energy and the annealing behavior, the EH5 acceptor level[21] at E_C−1.13 eV observed by DLTS in electron-irradiated *n*-type 4*H*-SiC after annealing at 750 °C seems to be a good candidate to the (1−|2−) level of V_CC_{Si}.

Figure 4(a) shows EPR spectra of V_C^+ and V_{Si}^- measured in dark at 77 K in HPSI 4*H*-SiC irradiated with electrons (dose, 2×10^{18} cm^{-3}) and annealed at 850 °C. This suggests that the (0|−) level of V_{Si} lies below the (+|0) level of V_C. The neutral divacancy, $V_CV_{Si}^0$, was not detected in the dark at 77 K in the same sample whereas at room temperature, the $V_CV_{Si}^0$ signal can be weakly detected in the dark [Fig. 4(b)]. This indicates that the (0|−) level of the divacancy may lie slightly below the (+|0) level of V_C at the cubic lattice site [at ~E_V+(1.47±0.06) eV (Ref. 22)] so that at room temperature

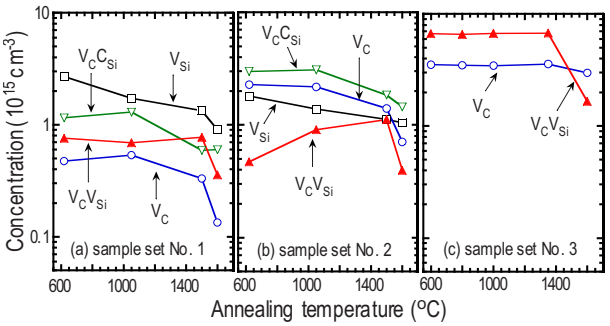

FIG. 5. (Color online) Annealing behavior of intrinsic defects in different types of HPSI 4*H*-SiC substrates: (a) sample set No. 1 with $E_a \sim 0.8-0.9$ eV, (b) sample set No. 2 with $E_a \sim 1.1-1.3$ eV, and (c) sample set No. 3 with $E_a \sim 1.5$ eV.

it could be partly thermally ionized and changed to the neutral charge state. This is supported by recent supercell calculations[15] which predicted the $(0|-)$ level to be at $\sim E_V + 1.4$ eV. Since the EPR signal of the divacancy is commonly observed in as-grown and irradiated samples, its $(0|-)$ acceptor level should be detectable by DLTS. In the whole region between 1.4–1.7 eV below E_C, there is only one reported DLTS level that is the *EH*6/7 level at $E_C - 1.65$ eV in irradiated samples[21,23] or at $E_C - 1.55$ eV in *n*-type 4*H*-SiC grown by CVD.[24] The similarity in the ionization energy and capture cross section as well as the annealing behavior suggests that the *EH*6/7 level originates from the same defect that gives rise to the RD_4 level at 1.49–1.60 eV below E_C in implanted materials[25] or the IL_6 level at ~1.45–1.55 eV below E_C in *n*-type 4*H*-SiC grown by PVT.[6] Taking into account the narrowing of the band gap at the measured temperatures[26] (~3.15 eV at ~650 K), the *EH*6/7 level is close to $\sim E_V + 1.5$ eV. In irradiated materials the *EH*6/7 peak contains two overlapping components[21,23] with one being annealed out at ~950 °C.[23] In our electron-irradiated HPSI 4*H*-SiC, the EPR signals of the divacancy *P*6/*P*7 centers start decreasing at temperatures ~850 °C, but did not completely disappear after annealing at ~1000 °C. However, in irradiated *n*-type 6*H*-SiC, the *P*6-related photoluminescence signals were already annealed out at temperatures ~1050 °C.[27] As suggested from our EPR experiment, the $(0|-)$ level of the divacancy lies very close to the $(+|0)$ level of V_C. Their DLTS signals are therefore expected to overlap with each other. Based on the energy position and the annealing behavior, the *EH*6/7 appears to be the best candidate for these two deep centers. Depending on the relative concentration between V_C and V_CV_{Si}, the DLTS peak may have different shape and appear at slightly different temperatures corresponding to different ionization energies. If the concentrations of V_C and V_CV_{Si} are similar or both are low but significantly different, then the resulting DLTS peak may appear as a single peak with the ionization energy varying depending on the relative concentration between the two centers. These seem to be the cases of the IL_6 center in *n*-type PVT substrates[6] and *EH*6/7 center in pure *n*-type CVD layers.[24] In electron-irradiated samples, the concentrations of both V_C and V_CV_{Si} are high, but are different enough to give rise to the *EH*6/7 DLTS peak consisting of two recognizable components.[21,23] The assignment of the *EH*6/7 center to the $(+|0)$ level of V_C and the $(0|-)$ level of V_CV_{Si} could explain the EPR and DLTS data. However, further investigations on the defect formation are needed for a conclusive identification.

In our estimation of the energy level of different charge states of V_CC_{Si} and V_CV_{Si}, it was not possible to distinguish between defect configurations corresponding to different inequivalent lattice sites and/or different symmetries.

C. High temperature annealing and stability of semi-insulating properties

The thermal stability of intrinsic defects was intensively studied, but mainly in irradiated materials. Their annealing behavior in as-grown materials is much less known. With low concentrations of impurities and intrinsic defects and without interstitial defects the annealing behavior of vacancies and vacancy-related complexes is expected to be different from that in irradiated materials. In this work, we study the annealing behavior of dominating defects (vacancies, divacancy, and carbon vacancy-carbon antisite defects) and their interaction at high temperatures as well as the stability of SI properties in different types of HPSI substrates. We choose three sets of samples based on the activation energy as classified in the preceding section. The sample set No.1 is initially characterized by $E_a \sim 0.8-0.9$ eV with concentrations of intrinsic defects: $n[V_{Si}] \sim 2-3 \times 10^{15}$ cm^{-3}, $n[V_CC_{Si}] \sim 1 \times 10^{15}$ cm^{-3}, $n[V_C]$ and $n[V_CV_{Si}]$ are in the mid-10^{14} cm^{-3} ranges [Fig. 5(a)]. The samples in the set No. 2 have initially $E_a \sim 1.1$ eV or ~1.25–1.28 eV with concentrations of vacancies and vacancy-related complexes: $n[V_{Si}] \sim 1-2 \times 10^{15}$ cm^{-3}, $n[V_C]$ and $n[V_CC_{Si}]$ are about $\sim 2-4 \times 10^{15}$ cm^{-3} and $n[V_CV_{Si}] \sim 6 \times 10^{14}$ cm^{-3} [Fig. 5(b)]. In the sample set No. 3, initially $E_a \sim 1.5$ eV, $n[V_C] \sim 3-4 \times 10^{15}$ cm^{-3}, and $n[V_CV_{Si}] \sim 5-6 \times 10^{15}$ cm^{-3} [Fig. 5(c)], whereas the V_{Si}^- and $V_CC_{Si}^-$ signals are not detectable by EPR (their concentrations may be in the low 10^{14} cm^{-3} ranges or less). SIMS measurements show the concentration of N to be $\sim 7 \times 10^{15}$ cm^{-3} in some samples and in the mid-10^{15} cm^{-3} ranges in most of the samples (the SIMS detection limit for N is also in the mid-10^{15} cm^{-3} ranges and varies from analysis to analysis). The concentration of B varies in the $1-3 \times 10^{15}$ cm^{-3} ranges. Here the EPR measurements were separately optimized for detecting different defects in each sample. The signals of V_{Si}^- and $V_CV_{Si}^0$ were always detected under illumination with light of photon energies ~2.0–2.8 eV; the $V_CC_{Si}^-$ signal was measured in dark after exposing the sample to light illumination whereas the V_C^+ signal was detected under illumination in sample sets No. 1 and No. 2 and in darkness in the sample set No. 3. The concentrations of defects were estimated from the intensities

of their EPR signals taking into account the number of defect configurations.

Annealing behaviors of common defects in the three sets of samples are shown in Fig. 5. In the sample set No. 1, V_{Si} and $V_C C_{Si}$ are the only two dominating defects. Their concentrations are not so high ($\sim 2-3\times 10^{15}$ cm^{-3} for V_{Si} and $\sim 1\times 10^{15}$ cm^{-3} for $V_C C_{Si}$) and individually they are not enough to compensate the N donors (n[N]–n[B]$\sim 4-5\times 10^{15}$ cm^{-3}). The V_C and $V_C V_{Si}$ defects have too low concentrations and cannot play an important role in carrier compensation in this case. Therefore, it is likely that the SI behavior in these samples is caused by V_{Si} and $V_C C_{Si}$. The *I-V* measurements showed the characteristics of *n*-type conduction which indicates that the Fermi level lies at ~0.85 eV below the conduction band minimum. This low activation energy seems to indicate that not only the single acceptor levels of V_{Si} and $V_C C_{Si}$ but also their higher negative charge states may be filled. According to the supercell calculations by Torpo *et al.*,[28] the $(2-|3-)$ and $(3-|4-)$ levels of V_{Si} lie at ~1.0–1.1 eV and ~0.6 eV, respectively, in the band gap of 4*H*-SiC. Among the reported DLTS levels, the *EH*2 level[21] at $E_C-0.68$ eV has similar annealing behavior as V_{Si} in irradiated material,[12] i.e., being annealed out at ~750 °C, and is a possible candidate for the $(3-|4-)$ level of V_{Si} although the measured capture coefficient seems to be too high. It is possible that the activation energy $E_a\sim 0.85$ eV is related to either the $(1-|2-)$ levels of $V_C C_{Si}$ or the $(2-|3-)$ level of V_{Si}. After annealing at 1600 °C, E_a was reduced to ~0.6 eV. These energy levels may be related to the $(3-|4-)$ levels of different configurations of V_{Si} which were being filled when the total concentrations of V_{Si} and $V_C C_{Si}$ were reduced [Figs. 5(a) and 5(b)]. The reduction of the concentration was observed for all defects (V_{Si}, V_C, $V_C C_{Si}$, and $V_C V_{Si}$). In addition, the transformation between V_{Si} and $V_C C_{Si}$ during high temperature annealing could also be seen [Fig. 5(a)]. With low concentrations of V_C, the formation of the divacancy via the interaction $V_C+V_{Si}\rightarrow V_C V_{Si}$ is an inefficient process [Fig. 5(a)].

In the sample set No. 2, the concentrations of V_C and $V_C C_{Si}$ are high. The single and double negative charge states of V_C is predicted by supercell calculations to be close to each other at ~1.0–1.17 eV and at ~0.85–1.05 eV below the conduction band,[28] respectively. The negatively charged carbon vacancy (V_C^-) was identified recently and photo-EPR experiments in irradiated 4*H*-SiC (Ref. 29) suggested that the $(1-|2-)$ level of V_C may be located at $\sim E_C-1.1$ eV. Comparing the *g* values we believed that the SI-6 center in HPSI 4*H*-SiC (Ref. 10) is the V_C^- center. Our previous photo-EPR experiments[11] indicated that the $(0|-)$ level of SI-6 (or V_C^-) may be at $\sim E_C-1.1$ eV or deeper if there is a Franck-Condon shift. In bulk growth, the concentration of the N donors in a wafer often varies with slightly higher doping levels in the center. In the parts with lower concentrations of N, it is possible that electrons may fill up to the $(0|-)$ level of $V_C C_{Si}$ at the energy range $\sim E_C-(1.24-1.4)$ eV, resulting in activation energies $E_a\sim 1.25-1.28$ eV as measured before annealing for some samples in the set No. 2. For higher concentrations of N, the $(0|-)$ and $(1-|2-)$ levels of V_C and $(1-|2-)$ level of $V_C C_{Si}$ may also be filled and E_a will be reduced (to ~1.1 eV in this case). It is difficult to distinguish if the activation energy $E_a\sim 1.1$ eV is related to the acceptor levels of V_C or $V_C C_{Si}$ since both the defects have high concentrations. We observed that after annealing at 1500 °C, E_a was reduced to $E_a\sim 0.74$ eV and was decreased further to ~0.6 eV after annealing at 1600 °C. After annealing the resistivity of both the sample sets No. 1 and No. 2 was reduced from $\sim 10^8-10^9$ Ω cm to $\sim 10^5$ Ω cm. With high concentrations of both V_C and V_{Si}, the interaction between the vacancies to form the divacancy was observed [Fig. 5(b)].

In the sample set No. 3, both V_C and $V_C V_{Si}$ have high concentrations. The observation of the strong V_C^+ signal in the dark indicates that the Fermi level lies below the $(+|0)$ level of V_C at ~1.5 eV above E_V. Therefore, higher lying acceptor levels of V_C will not be involved in the carrier compensation process. The B acceptors and the $(0|-)$ level of $V_C V_{Si}$ seem to be enough to compensate the N donors in these samples. Depending on the N concentration, the Fermi level can be pinned at different $(0|-)$ levels corresponding to four configurations of $V_C V_{Si}$ in 4*H*-SiC. If the concentration of N is low, only the deeper $(0|-)$ level of the divacancy may be filled and, consequently, a larger activation energy of $E_a\sim 1.6$ eV is obtained. For higher N concentrations, other higher lying $(0|-)$ levels corresponding to shallower configurations of the divacancy may also be filled, resulting in smaller activation energies of $E_a\sim 1.4-1.5$ eV. This may explain the map of the activation energy in PVT substrates[6,7] with the values $E_a\sim 1.55-1.6$ eV observed only near the edge of the wafer, where the N concentration is often lower, and $E_a\sim 1.4-1.5$ eV in the typically higher-doping center region of the wafer. After annealing at 1600 °C, the concentration of V_C is only slightly decreased whereas the reduction of the divacancy concentration is more pronounced [Fig. 5(c)]. We also found that E_a reduced from ~1.53 eV to ~1.06 eV but the resistivity was still $\geqslant 10^9$ Ω cm. The divacancy concentration is reduced to $\sim 1.5\times 10^{15}$ cm^{-3}. Together with the B acceptors (n[B]$\sim 3\times 10^{15}$ cm^{-3}) the divacancy is not enough to compensate the N donors (n[N]$\sim 5\times 10^{15}$ cm^{-3}), leading to the electron occupancy of the higher lying $(0|-)$ and $(1-|2-)$ levels of V_C, which may be at $\sim E_C-1.1$ eV as shown above. This explains the change of E_a from ~1.53 eV to ~1.06 eV. If the total concentration of the divacancy and B acceptors is still larger than that of the N donors, the Fermi level and hence E_a remains unchanged as seen in some HPSI SiC samples grown by HTCVD.[4,5] The result also indicates that the concentration of the divacancy estimated by EPR under light illumination in this case ($\sim 1.5\times 10^{15}$ cm^{-3}) is not much lower than its real concentration, otherwise the total acceptor concentration would be enough to compensate the N donors and keep E_a unchanged.

The annealing behavior of V_C in the sample set No. 3 [Fig. 5(a)] is clearly different from that in the sample sets No. 1 and No. 2 [Figs. 5(a) and 5(b)]. In absence of V_{Si}, the process $V_C+V_{Si}\rightarrow V_C V_{Si}$ does not occur. The migration of V_C via the nearest neighbors to form vacancy-antisite pairs is unlikely since $V_{Si}Si_C$ is predicted to be unstable.[30] Therefore, in the sample set No. 3, V_C is more thermally stable.

As shown above, dominating defects in HPSI SiC are V_{Si}, V_C, $V_C C_{Si}$, and $V_C V_{Si}$, each having several deep acceptor

levels in the band gap. Depending on the concentrations of N donors and B acceptors, some or all of these acceptor levels may be involved in the carrier compensation processes. In sample sets No. 1 and No. 2, the concentrations of intrinsic defects are in the range of $\sim 1-4\times 10^{15}$ cm^{-3} and reduce to $\sim 1\times 10^{15}$ cm^{-3} or less after 1600 °C annealing. Therefore, shallower acceptor levels should be filled, leading to lower activation energies and hence lower resistivities. Even in cases when the N concentration can be reduced further to avoid the reduction of the resistivity of substrates, V_{Si} and also $V_C C_{Si}$, which can transform back to V_{Si} at high temperatures, are not desirable defects for controlling SI properties since its several highly negatively acceptor states, possibly located at $\sim E_C-(0.6-0.9)$ eV, will also work as carrier traps, worsening the performance of high-frequency devices. In these samples, with the presence of V_{Si}, the interaction between V_C and V_{Si} to form the divacancy is enhanced and consequently V_C becomes less thermally stable similar to V_{Si}, $V_C C_{Si}$, and the divacancy.

IV. CONCLUSION

The V_{Si}, V_C, $V_C C_{Si}$, and $V_C V_{Si}$ centers are found to be common defects in different types of HPSI SiC substrates with the concentrations varying from low-10^{14} cm^{-3} to low- and mid-10^{15} cm^{-3}. HPSI substrates can be classified into three types characterized by the thermal activation energy $E_a \sim 0.8-0.9$ eV, $\sim 1.1-1.3$ eV, and ~ 1.5 eV. The energy positions of some deep acceptor levels of $V_C C_{Si}$ and $V_C V_{Si}$ were estimated by EPR and photo-EPR experiments. The V_{Si} center is found to be the dominating defect in HPSI substrates with $E_a \sim 0.8-0.9$ eV and this activation energy may be related to the $(2-|3-)$ acceptor level of V_{Si}. In substrates with $E_a \sim 1.1-1.3$ eV, the $V_C C_{Si}$ and V_C centers are dominating defects. The $(0|-)$ level of $V_C C_{Si}$ was estimated by photo-EPR to be in at $\sim 1.24-1.4$ eV below E_C. This level is possibly related to the activation energy $E_a \sim 1.25-1.3$ eV. The $(1-|2-)$ level of $V_C C_{Si}$ may be related to the energy threshold at ~ 1.05 eV. However, without knowledge on Franck-Condon shifts and possible involvements of indirect optical transitions, the estimated energy position should be considered as preliminary. In samples with dominating signals of both V_C and $V_C C_{Si}$, it is still not clear if the activation energy $E_a \sim 1.1$ eV is also related to acceptor levels V_C or to the $(1-|2-)$ level of $V_C C_{Si}$.

Based on EPR experiments performed at different temperatures, the $(0|-)$ level of $V_C V_{Si}$ was estimated to be located at slightly below the $(+|0)$ level of V_C at ~ 1.5 eV above the valence band. The thermal transition between the $(0|-)$ level of $V_C V_{Si}$ and the conduction band occurring at temperatures 600–700 K could explain the activation energy $E_a \sim 1.5$ eV often observed in samples with dominating signals of V_C and $V_C V_{Si}$. The activation energy $E_a \sim 1.1$ eV observed after annealing in this sample set may be associated to the $(0|-)$ and/or $(1-|2-)$ levels of V_C. The energy separation between these two charge states is not known.

The decrease of the concentrations of V_{Si}, V_C, $V_C C_{Si}$, and $V_C V_{Si}$ defects after high temperature annealing was observed in all types of HPSI substrates. This leads to the decrease of the activation energy (to ~ 0.6 eV) and the resistivity (to $\sim 10^5 \Omega$ cm) in samples with dominating V_{Si} and $V_C C_{Si}$ defects. In samples with dominating V_C and $V_C V_{Si}$ defects, the V_{Si} and $V_C C_{Si}$ centers were absent and V_C becomes more thermally stable. The activation energy was also reduced to ~ 1.1 eV, but it is deep enough to keep the resistivity unchanged.

From the annealing studies, it is suggested that V_C and the divacancy are suitable defects for controlling the SI properties in SiC. However, V_C is stable only when V_{Si} is absent or present with a negligible concentration. Optimizing the crystal growth conditions to minimize the formation of V_{Si} is therefore important.

ACKNOWLEDGMENTS

Support from the Swedish Foundation for Strategic Research program SiCMAT, the Swedish Research Council, and the Swedish National Infrastructure for Computing is acknowledged. The authors thank Cree Inc. for HPSI SiC samples.

[1] M. Bhatnagar and B. J. Baliga, IEEE Trans. Electron Devices **40**, 645 (1993).
[2] H. McD. Hobgood, M. F. Brady, M. R. Calus, J. R. Jenny, R. T. Leonard, D. P. Malta, A. R. Powell, V. F. Tsvetkov, R. C. Glass, and C. H. Carter, Jr., Mater. Sci. Forum **457-460**, 3 (2004).
[3] A. Ellison, B. Magnusson, B. Sundqvist, G. Pozina, J. P. Bergman, E. Janzén, and A. Vehanen, Mater. Sci. Forum **457-460**, 9 (2004).
[4] A. Ellison, B. Magnusson, C. Hemmingsson, W. Magnusson, T. Iakimov, L. Storasta, A. Henry, N. Henelius, and E. Janzén, Mater. Res. Soc. Symp. Proc. **640**, H1.2 (2001).
[5] A. Ellison, B. Magnusson, N. T. Son, L. Storasta, and E. Janzén, Mater. Sci. Forum **433-436**, 33 (2003).
[6] St. G. Müller, M. F. Brady, W. H. Brixius, R. C. Glass, H. McD. Hobgood, J. R. Jenny, R. T. Leonard, D. P. Malta, A. R. Powell, V. F. Tsvetkov, S. T. Allen, J. W. Palmour, and C. H. Carter, Jr., Mater. Sci. Forum **433-436**, 39 (2003).
[7] J. R. Jenny, D. P. Malta, M. R. Calus, St. G. Müller, A. R. Powell, V. F. Tsvetkov, H. McD. Hobgood, R. C. Glass, and C. H. Carter, Jr., Mater. Sci. Forum **457-460**, 35 (2004).
[8] M. E. Zvanut and V. V. Konovalov, Appl. Phys. Lett. **80**, 410 (2002).
[9] W. E. Carlos, E. R. Glaser, and B. V. Shanabrook, Physica B **340-342**, 151 (2003).
[10] N. T. Son, B. Magnusson, Z. Zolnai, A. Ellison, and E. Janzén, Mater. Sci. Forum **433-436**, 45 (2003).
[11] N. T. Son, B. Magnusson, Z. Zolnai, A. Ellison, and E. Janzén, Mater. Sci. Forum **457-460**, 437 (2004).
[12] E. Sörman, N. T. Son, W. M. Chen, O. Kordina, C. Hallin, and E. Janzén, Phys. Rev. B **61**, 2613 (2000).

[13] N. Mizuochi, S. Yamasaki, H. Takizawa, N. Morishita, T. Ohshima, H. Itoh, T. Umeda, and J. Isoya, Phys. Rev. B **72**, 235208 (2005).
[14] V. S. Vainer and V. A. Il'in, Sov. Phys. Solid State **23**, 2126 (1981).
[15] N. T. Son, P. Carlsson, J. ul Hassan, E. Janzén, T. Umeda, J. Isoya, A. Gali, M. Bockstedte, N. Morishita, T. Ohshima, and H. Itoh, Phys. Rev. Lett. **96**, 055501 (2006).
[16] N. T. Son, P. N. Hai, and E. Janzén, Phys. Rev. B **63**, 201201(R) (2001).
[17] T. Umeda, N. T. Son, J. Isoya, E. Janzén, T. Ohshima, N. Morishita, H. Itoh, A. Gali, and M. Bockstedte, Phys. Rev. Lett. **96**, 145501 (2006).
[18] W. E. Carlos, E. Glaser, B. V. Shanabrook, and T. A. Kennedy, Bull. Am. Phys. Soc. **48**, 1132 (2003).
[19] J. Franck, Trans. Faraday Soc. **21**, 536 (1925).
[20] E. U. Condon, Phys. Rev. **32**, 858 (1928).
[21] C. G. Hemmingsson, N. T. Son, O. Kordina, P. J. Bergman, E. Janzén, J. L Lindström, S. Savage, and N. Nordel, J. Appl. Phys. **81**, 6155 (1997).
[22] N. T. Son, B. Magnusson, and E. Janzén, Appl. Phys. Lett. **81**, 3945 (2002).
[23] L. Storasta, J. P. Bergman, E. Janzén, A. Henry, and J. Lu, J. Appl. Phys. **96**, 4909 (2004).
[24] K. Danno, T. Kimoto, and H. Matsunami, Appl. Phys. Lett. **86**, 122104 (2005).
[25] T. Dalibor, G. Pensl, H. Matsunami, T. Kimoto, W. J. Choyke, A. Schöner, and N. Nordel, Phys. Status Solidi A **162**, 199 (1997).
[26] W. J. Choyke, Mater. Res. Bull. **4**, S141 (1969).
[27] M. V. B. Pinheiro, E. Rauls, U. Gerstmann, S. Greulich-Weber, H. Overhof, and J.-M. Spaeth, Phys. Rev. B **70**, 245204 (2004).
[28] L. Torpo, M. Marlo, T. E. M. Staab, and R. M. Nieminen, J. Phys.: Condens. Matter **13**, 6203 (2001).
[29] T. Umeda, Y. Ishitsuka, J. Isoya, N. T. Son, E. Janzén, N. Morishita, T. Ohshima, H. Itoh, and A. Gali, Phys. Rev. B **71**, 193202 (2005).
[30] A. Mattausch, M. Bockstedte, and O. Pankratov, Mater. Sci. Forum **353-356**, 323 (2001).